Dry Drilling Performance Enhancement using Optimized Diamond-Like Carbon Coatings

Eyob Messele (Eyob.Messele@bdu.edu.et)
National Taiwan Institute of Technology: National Taiwan University of Science and Technology
https://orcid.org/0000-0003-4660-6262
Vijaykumar S Jatti
Ashwini V. Jatti
Akshansh Mishra
Rahul Dhabale

Research Article

Keywords: Plasma Enhanced Chemical Vapor Deposition, Diamond-Like-Carbon, Surface roughness, Spindle Load, Optimization, Coating

Posted Date: November 8th, 2022

DOI: https://doi.org/10.21203/rs.3.rs-2208937/v1

Version of Record: A version of this preprint was published at The International Journal of Advanced Manufacturing Technology on June 22nd, 2023. See the published version at https://doi.org/10.1007/s00170-023-11794-3.

Abstract

This study demonstrates the performance enhancement of drill bits during dry cutting operation of LM6 aluminum alloy and bright mild steel using optimized Diamond-Like-Carbon (DLC) coatings. DLC coatings are deposited using Plasma Enhanced Chemical Vapour Deposition (PECVD) process by varying the process parameters, bias voltage, bias frequency, gas mixture, and working pressure. DLC coatings were grown over the silicon, high-speed steel, and stainless-steel pin substrate. Coating's chemical, composition, topography, and mechanical properties measurements were checked using Fourier Transform Infrared (FTIR), micro-Raman spectroscopy, Atomic Force Microscopy, and intrinsic stress & nano-hardness/micro-hardness tester, respectively. Coating deposition and optimization were carried out as per the Taguchi method. Further, the optimized DLC coatings tribological test and the effect of DLC coating on the tool life were performed. Results showed that the DLC-coated substrate had less wear loss and coefficient of friction than the uncoated substrate. The dry-cutting test showed that coated drill bits produce a better surface finish and consume less power in the drilling operation than uncoated drill bits. This is due to the low coefficient of friction and low wear loss of the DLC coatings.

1. Introduction

Diamond-Like-Carbon (DLC) coatings are amorphous carbon-based coatings with a high hardness and a low coefficient of friction; thus, it is a promising material for tribological application [1]. DLC films initially found application in improving the tribology of magnetic head sliders and magnetic storage media. In recent years, there has been more emphasis on applying DLC films to mass-produced mechanical components, particularly in the automotive sector, such as gears, bearings, pistons rings, shafts, cam/tappets, rocker shafts, and roller pins. DLC also found application in biomedical areas such as coating for hip joints and knee replacement. Application in manufacturing industries includes plastic molds, extrusion dies, stamping devices, and cutting tools. Manufacturers ensure the economical mass production of cutting tools by applying thin film coatings onto the cutting tools, which have low friction and prevent the sticking of metal on the tool surfaces; otherwise, it leads to increased power consumption, tool wear, and material property changes [2]. Manufacturers use available commercial coatings to enhance tool life and improve cutting efficiency. Many tool manufacturers produce tools using coatings of oxides, ceramics, carbides, and titanium nitrides. Below are some published works on the deposition and tribology of DLC coatings and their application in cutting tools. Conrads and Schmidt [3] reviewed the most commonly used methods for the generations of plasma with special emphasis on non-thermal, low-temperature plasma for technological applications.Psyllaki, et al. [4] studied tribological behavior and the wear mechanisms of 2 μm thick DLC coatings by the Pin-On-Disc testing method. Dorner, et al. [5] studied the influence of the coating thickness on the structure and the abrasive wear resistance of DLC of 0.7, 1.5, and 3μm thick coatings deposited on Ti6Al4V. Pauschitz, et al. [6] compared mechanical properties such as hardness, elastic modulus, and surface roughness of thin DLC films deposited by the PECVD process and the unbalanced magnetron sputter deposition process. KAGIYA [7] developed high-adhesion and low friction DLC coating for cutting tools for machining aluminum material.

Fukui, et al. [8] studied the impact of tribological properties of DLC-coated tools on cutting performance. Lee [9] applied inductively coupled plasma to lower the process temperature of CVD and PVD without sacrificing the deposition rate and the film qualities. Irmer and Dorner-Reisel [10] conducted micro-Raman studies for DLC coatings. Raman scattering is a relatively easy, fast, and non-destructive method for the characterization of DLC, containing information about the carbon bonding sp3/sp2 ratio. Zaidi, et al. [11] characterized DLC coating deposited on stainless steel 304L adherence by scratch testing.

Bhowmick and Alpas [12] conducted experiments to check the performance of hydrogenated, non-hydrogenated DLC-coated tools, and uncoated tools during the dry drilling of 319Al and concluded that hydrogenated DLC-coated drills provide better dry drilling performance than non-hydrogenated DLC coated tools and uncoated one. Zolgharni, et al. [13] showed enhancements in cutting tools' performance and energy efficiency by the deposition of optimized DLC coatings on machine parts. Optimized deposition conditions produced drill bits with a 25% reduction in swarf clogging, a 36% reduction in power consumption and a 5 times increase in tool life. Dowling [14] provided an overview of how plasma-deposited coatings can significantly enhance the surface properties of metallic components. Cao, et al. [15] showed DLC films have smooth surfaces, homogeneous particle sizes, and excellent tribological properties, which can be used to improve the surface quality of the selenium drums and prolong their service life. Heinemann and Hinduja [16] investigated the feasibility of DLC-coated twist drills in deep-hole drilling and concluded that DLC coatings can potentially improve chip evacuation from deep holes and generate lower drilling torque. Suzuki, et al. [17] discussed the effect of the surface roughness of hydrogenated DLC films on friction and wear properties using a ball-on–disc type tribometer in air and water environments. Bhowmick and Alpas [18] investigated the performance of non-hydrogenated DLC (NH-DLC) coated HSS drills during the drilling of cast magnesium alloy (AZ91) under dry and Minimum quantity water lubrication. Kumar, et al. [19] deposited DLC coating using the PECVD method of 3 μm and 10 μm thick on stainless steel disk and ring specimens. They found that 10 μm coating has more wear resistance. Pang, et al. [20] deposited DLC films on p-type Si (100) substrates using the RF hollow cathode method and obtained a deposition rate of 45 nm/min deposition rate. The higher deposition rate is obtained at higher plasma density. Bewilogua and Hofmann [21] reported the research carried out by various researchers to develop a-C: H, ta-C, metal-containing a-C:H: Me, and non-metal-containing a-C: H:X coatings. They identified the reason for the hindrance of using DLC coating for industrial applications due to film thickness limitation and compressive stress developed in coatings. Waseem, et al. [22] worked on developing enhanced adhesion strength with good mechanical and tribological properties. Resulted in depicted adhesion showed the scratch mark at 20 N load. Hauert [23] developed DLC coating for automotive parts using the PECVD method and found reduced friction. Ye, et al. [24] studied the tribocorrosion of multilayer DLC coating grown over 304L stainless steel under seawater. They employed the magnetron sputtering method for developing multilayer DLC coating. Results showed the potential of using this coating for the marine industry. Bouabibsa, et al. [25] developed Me-DLC using the RF-PECVD method with Ar, H_2, C_2H_2, mixture with the addition of pure metal (Al, Ti, Nb) by magnetron sputtering. Results showed that adding metallic elements leads to disorder within the carbon matrix. Liu, et al. [26] deposited DLC coatings on nitrile butadiene rubber substrates using magnetron sputtering. They

investigated the effect of Ar sputtering pressure on tribology performance, wettability, structure, and surface topography of the DLC coating. Results exhibited enhanced trio performance of DLC coatings under 1.4 Guo, et al. [27] developed multilayer hydrogen-free DLC coatings, namely, a-C:X in a-C/a-C:X, a-C/a-C:Si, a-C/a-C and a-C:X monolayers. Results exhibited that multilayer (a-C:X) DLC coatings have good tribo-mechanical properties. Claver, et al. [28] developed ta-C and WC-C DLC coatings on three tool steel, K360, vanadis 4, and vancron, using the HiPIMS method with positive pulses. Results exhibited excellent tribological properties in terms of resistance to wear / adhesion. Bai, et al. [29] deposited DLC coatings on a rubber substrate to obtain ultralow friction, high hardness, and chemical compatibility with rubber. The authors reported that optimum tribological performance was obtained when 29% hydrogen-containing DLC was coated on rubber.

The literature concluded that the properties of DLC coating depend significantly on the coating process parameters. As the deposition of DLC coatings by PECVD involves several process parameters, the present work aims to optimize the PECVD process by using the Taguchi approach. In this study, DLC coatings are grown on a p-type silicon wafer, HSS substrate, SS wear pins and HSS Drill Bits. Composition, Chemical, Mechanical, Topographical and Tribological properties of the coatings are characterized and evaluated by Fourier transform infrared spectroscopy, Raman spectroscopy, Nano-Hardness tester, Atomic force microscopy, and pin-on-disc tribometer. The optimized DLC coating's performance was tested for dry drilling applications. The purpose of using DLC coating on the drill bit is to achieve low friction tool surface, avoid built-up edge, enhance passing, and remove metal swarf through the helical drill form. Cutting tests were performed for uncoated and coated drill bits on LM6-aluminum alloy and Bright mild steel under dry drilling conditions to study the effect of DLC coating on the tool life.

2. Materials And Methods

2.1. DLC Coating Deposition

The Plasma Enhanced Chemical Vapour Deposition (PECVD) system used in the present study consists of a semi-circular vacuum chamber made of SS 304L with a front opening door; refer to Fig. 1a for a schematic diagram of the PECVD process. The high vacuum of the order 10^{-6} bar is achieved by combining a molecular turbopump and a backing rotary pump. The penning gauge measures the high vacuum, and roughing vacuum is measured by the Pirani gauge. MKS measures process gas pressure make a capacitance manometer (Baratron) with a power supply and display unit, and the process gas flow is controlled and monitored by MKS make gas handling system. The plasma is generated by a 500 Watt, 13.56MHz frequency RF power supply with an auto-matching network with water-cooled RF feed. The cleaned substrates were placed in the PECVD chamber, and the chamber was pumped down to a vacuum of $5x10^{-6}$ bar using a combination of rotary and turbo pumps. Then the vacuum chamber was purged with methane and hydrogen to avoid contamination of the coating. After purging, the substrates were cleaned using hydrogen plasma for ten minutes. After the etching process, process gas mixtures,

methane, and hydrogen were allowed into the chamber in the chosen ratio, and plasma was created with an RF power of 50 watts. Magpul did substrate biasing to make a DC-Pulsed power supply. The pulse generated by this supply is symmetrical bipolar, i.e., the positive and negative voltages are equal, as shown in Fig. 1b.

2.2. Substrates Used

The present study uses five types of substrates, i.e., boron-doped p-type (100) silicon, 20 mm x 20 mm, 500 microns thick with 1–10Ωcm resistivity; 2 mm thick High-Speed Steel (HSS, M42, 8% cobalt); Stainless Steel (SS304L) wear pin of Dia10 mm x 25 mm length; and HSS drill bits of Dia 5mm, 52 mm flute length, 86 mm overall length, Parallel shank, Jobber series, Addison make.

2.3. Experimental Design

Figure 2 shows the cause and effect diagram for the deposition of DLC film in a typical PECVD process. As can be seen, several process parameters influence the process and the resulting film structure and properties. The parameters for depositing DLC by Plasma Enhanced Chemical Vapour Deposition (PECVD) process are bias voltage, bias frequency, RF power, gas mixture, pressure, substrate temperature, and coating time.

In this study Taguchi L_9 (3^4) orthogonal array was used for the experimental layout for the deposition parameters. This array consists of four control parameters and three levels, as shown in Table 1. In the Taguchi method, all observed values are calculated based on “bigger is best” and “smaller is best.” Thus, in this study, the Hardness and Id/Ig ratio experimental values were set too high and low, respectively. Analysis of variance (ANOVA) and F-test (Standard analysis) are used to analyze the experimental data to identify the most significant parameters. Experiments were carried out per the designed layout, as shown in Table 2.

Table 1
Deposition parameters and their levels for DLC coatings

Control Parameters	Level			Observed Values
	1	2	3	
	Low	Medium	High	
Bias Voltage, V(volt)	-50	-150	-500	1. Hardness (GPa)
Bias Frequency, F (kHz)	0.5	10	60	
Deposition Pressure, P (μbar)	2	4	6	2.I_D/I_G ratio
Gas Composition, G (%)	60:40	80:20	90:10	

Table 2
Experimental Details

Exp. No.	Bias Voltage (Volts)	Bias Frequency (KHz)	Deposition Pressure (µbar)	Gas Composition (%)
D80	-50	0.5	2	60:40
D77	-50	10	4	80:20
D72	-50	60	6	90:10
D81	-150	0.5	4	90:10
D75	-150	10	6	60:40
D73	-150	60	2	80:20
D82	-500	0.5	6	80:20
D76	-500	10	2	90:10
D74	-500	60	4	60:40

2.4. Characterization of DLC Coatings

Non-destructive techniques like Fourier Transform Infrared Spectroscopy, micro–Raman Spectroscopy, and Atomic Force Microscopy characterize the composition, chemical properties, and topography. Destructive techniques like Nano-Hardness testing and wear testing using a Pin-on-disc tribometer describe mechanical and tribological properties.

2.5. Fourier Transform Infrared Spectroscopy (FTIR)

IR spectrum of DLC films was obtained using VECTOR 22 FTIR spectrometer (BRUCKER make), by measuring the radiation absorption bands in the range of 2600–3300 cm^{-1}, where the absorption bands of the sp^3 and sp^2 bonded carbon in the C-H group.

2.6. Raman Spectroscopy

The Raman spectra of the coatings were obtained using the Micro Raman spectrometer Labram 010 Model of DILOR-JOBIN-SPEX. The source was a He-Ne laser of wavelength 632nm and 3mW power. The obtained Raman spectra were fitted with two Gaussian curves after subtracting a linear background. The ratio I_D/I_G was obtained by computing the areas of D-peak and G-peak and taking their ratio.

2.7. Atomic force microscopy

The topography and surface roughness (Ra) of DLC films are obtained by contact mode using Surface Imaging Systems Atomic Force Microscopy (AFM). The area of scanning used for AFM analysis is 5µm x 5 µm and 10µm x 10µm.

2.8. Intrinsic Stress Measurement

The intrinsic stress in DLC films is the major component of residual stresses; the magnitude of residual stresses is most commonly calculated by the curvature method based on measurements of the deformation of film-substrate structures [30]. The magnitude of residual stresses (σ) is deduced from measurements of the radius of curvature (R_1) of the initial substrate and the radius of curvature (R_2) of the substrate covered with the film. The curvature radii were determined by surface Profilometer measurements and two-beam interferometer measurements. From Stoney's Eq. (1) [30]

$$\sigma = \frac{1}{6} * \left(\frac{E_s}{1-\nu_s}\right) * \frac{t_s^2}{t_f} * \left(\frac{1}{R_2} - \frac{1}{R_1}\right) \qquad (1)$$

Where E_s and v_s is the young's modulus and Poisson's ratio, t_s and t_f are the substrate and film thickness, respectively. Figure 3a shows the technique for measuring intrinsic stress build-up during deposition. Figure 3b Schematic representation of the stress measurement process. The radius of curvature (R) is determined for a measured displacement, d [30];

$$R \sim \frac{2Dl}{d} \qquad (2)$$

2.9. Hardness Measurement

For DLC coatings deposited on a silicon substrate, the nano hardness was measured by Nano-hardness Tester (CSEM Instruments) fitted with an integrated optical (Nikon)/Atomic Force Microscope (Surface Imaging Systems) equipped with a Berkovich diamond indenter, having a triangular-pyramid shape. In the case of HSS substrates, where the surface roughness was higher, the common micro hardness testers, namely, Vickers (micro Vickers) and the Knoop hardness, were used to measuring the coating hardness. Generally, Knoop hardness is used for thinner films, as the depth of indentation is relatively low compared to the Vickers test. A Buehler® make Micromet Testing Machine with Knoop indenter at load 25gf was used for coatings on HSS.

2.10. Tribological Properties

DLC coatings are often used to improve the wear resistance and durability of the engineering components. In order to determine the performance of the coatings, many wear testing techniques are used. The two standards referring to the pin-on-disc tribometer are DIN 50324 – Testing of friction and wear and ASTM G99-95a – standard test method for wear testing with a pin-on-disc apparatus. The present study follows the ASTMG99-95a standard test methodology [31]. The wear rate and coefficient of friction of DLC films were estimated using a DUCOM make Wear and Friction Monitor, model TR201. Testing parameters were: load – 500 grams, disc speed- 50 rpm, Relative humidity 40% with variable track radius.

2.11. Cutting Performance

Drilling experiments were conducted using a 3-axis CNC Machining Centre (DAHLIH 1202BA Vertical Machining Centre) to achieve consistent testing conditions. Drill bits were coated using a Magpuls DC power supply. Workpiece materials were LM6-aluminium alloy with a hardness of 50 BHN and Bright Mild Steel with a hardness of 120 BHN. The hole geometry was 5 mm in diameter and 12 mm deep blind. Drilling tests were conducted at a cutting speed of 60 m/min (3821 rpm), and a feed rate of 0.12 mm/rev (458 mm/min) for aluminum material, and bright mild steel cutting speed was set at 20 m/min (1,250 rpm) and feed rate of 0.06 mm/rev (75 mm/min). No lubrication was used, and the analysis of results focused on the spindle load during the drilling operation, the number of holes produced before drill failure, and the surface finish of the drilled holes. The surface roughness of drilled holes was measured by Contour and Roughness tester (Make-Taylor Hobson, Model-Form Talysurf Intra). Figure 4 depicts the experimental drilling setup. Drill bits wear measured using Lab make Tool-Makers Microscope.

3. Results And Discussion

3.1. Fourier Transform Infrared Spectroscopy

The characteristic FT-IR spectra of DLC films lie in the stretching modes in the 3100-2800cm^{-1} and a bending mode in the 1700-1300cm^{-1}range. The C-H absorption band in the 3100-2800cm^{-1} range corresponds to sp^3 and sp^2 bonded carbon. The spectra in the bending region are not shown here because of the background noise corresponding to the Si substrate. IR absorbance of DLC films was estimated by measuring the height of the peaks of each sample with the baseline correction as a first approximation. The values are tabulated in Table 3. The FT-IR results revealed that DLC films were partially hydrogenated, consisting of various sp^3 and sp^2-related C-H bonds. Three peaks are clearly observed in Fig. 6, at 2969cm^{-1}, 2924cm^{-1} and 2854cm^{-1}.

Table 3
IR absorbance value for DLC film

Sl. No.	IR absorbance at 2969cm^{-1}	IR absorbance at 2924cm^{-1}	IR absorbance at 2854cm^{-1}
D72	0.643	0.762	0.452
D73	0.742	0.968	0.565
D74	0.850	1.075	0.600
D75	0.75	0.975	0.550
D76	0.688	0.938	0.513
D77	0.650	0.900	0.525
D80	0.700	0.875	0.525
D81	0.655	0.836	0.545
D82	0.691	0.873	0.582

3.2. Raman Spectroscopy

The Raman spectrum obtained by Raman spectroscopy for DLC film is shown in Fig. 7 and Fig. 7. There are two peaks of interest. One peak is located at a wave number of 1360 cm^{-1} corresponding to the sp^3 carbon bond, known as the disorder peak. For diamond, with pure sp^3 bonding corresponding peak is located at 1330 cm^{-1}. The second peak is the sp^2 carbon bond located at a wave number of 1550 cm^{-1}. The peaks were fitted with two Gaussian peaks to estimate the I_D/I_G ratio. The I_D/I_G values were obtained from the ratio of the areas of the D-peak and the G-peak, and the same is tabulated in Table 4.

Table 4
ID/IG ratios of DLC films deposited on HSS and Silicon

Sl. No.	I_D/I_G ratio of DLC film deposited on HSS	I_D/I_G ratio of DLC film deposited on silicon
D72	0.96	0.5
D73	1.46	0.78
D74	1.45	0.54
D75	1.14	0.93
D76	3.00	1.02
D77	3.27	0.5
D80	1.09	1.63
D81	1.69	0.37
D82	1.59	0.54

3.3. Atomic Force Microscopy

Figure 8a and Fig. 8b show the DLC films' three-dimensional topography for the substrate and different DLC films coated on silicon samples. The area of scanning used for AFM analysis is 5μm x 5μm and 10μm x 10μm. The surface roughness value for bare silicon is 10 nm, whereas the range of DLC coatings lies between 6.9 nm to 9.0 nm. The AFM images and surface roughness values make the films smoother than the bare silicon.

3.4. Intrinsic Stress Measurement

The residual stress for DLC films is calculated per the formulae using equations (1) and (2), and the calculated values are tabulated in Table 5. It can infer from the table that film stresses are both tensile and compressive in nature.

Table 5
Intrinsic stress values for DLC films

Experimental parameters (Bias Voltage, Bias Frequency, Pressure and Gas composition)	R_1 (m)	R_2 (m)	t_f (µm)	Stress (MPa)
50V,500Hz,2µbar,60:40	-48.16	-256.30	0.55	551.2
50V,10KHz,4µbar,80:20	1.20	52.94	0.5	12200
50V,60KHz,6µbar,90:10	83.72	-177.02	0.9	-147
150V,500Hz,4µbar,90:10	-269.16	-911.63	0.6	32.82
150V,10KHz,6µbar,60:40	-15.91	-24.79	0.63	268
150V,60KHz,2µbar,80:20	16.59	442.60	0.7	-623.3
500V,500Hz,6µbar,80:20	-124.06	-134.85	0.7	6.929
500V,10KHz,2µbar,90:10	38.21	216.75	0.8	-202.7
500V,60KHz,4µbar,60:40	-130.35	-335.15	0.6	58.76

3.5. Hardness Measurement

Hardness and Young's Modulus for DLC films were determined from indentation load-displacement data on silicon samples. The load versus displacement curve obtained for DLC film is illustrated in Fig. 9 at a maximum load of 5 mN and a maximum depth of indentation of 125 nm. The residual displacement was 50 nm for a total displacement of 125 nm. Thus, the film undergoes 60% elastic deformation and 40% plastic deformation. The hardness of the silicon substrate is 13.8 GPa. The hardness value for DLC film coated on HSS using a symmetric bipolar DC power supply was measured by a micro-hardness tester. The hardness value of the HSS substrate was 1212 KHN. Table 6 shows the hardness values for DLC films deposited on silicon and HSS substrate.

Table 6
Hardness values for DLC films deposited on HSS and Silicon

Experimental parameters (Bias Voltage, Bias Frequency, Pressure and Gas composition)	Hardness of DLC films deposited on HSS (KHN_{25gf})	Hardness of DLC films deposited on Silicon (GPa)
50V,500Hz,2µbar,60:40	1509	17.31
50V,10KHz,4µbar,80:20	1550	19.83
50V,60KHz,6µbar,90:10	1570	19.42
150V,500Hz,4µbar,90:10	1482	17.73
150V,10KHz,6µbar,60:40	1314	15.73
150V,60KHz,2µbar,80:20	1338	15.23
500V,500Hz,6µbar,80:20	1524	16.78
500V,10KHz,2µbar,90:10	1460	16.09
500V,60KHz,4µbar,60:40	1493	16.29

3.6. DLC Coatings Optimization

In this study, all the analysis based on the Taguchi method was done to determine the process parameters' main effects and establish the optimum conditions. The principal effect analysis was used to study the trend of the impact of each of the factors. Table 7 list the L-9 orthogonal array with observed values for ID/IG ratio and hardness on the HSS substrate.

Table 7
L9 (34) Orthogonal Array and Observed Values

Factors				Response of study	
Bias Voltage (Volts)	Bias Frequency (kHz)	Deposition Pressure (µbar)	Gas Composition (%)	I_D/I_G ratio	Hardness (KHN_{25gf})
-50	0.5	2	60:40	1.09	1509
-50	10	4	80:20	3.27	1550
-50	60	6	90:10	0.96	1570
-150	0.5	4	90:10	1.69	1482
-150	10	6	60:40	1.14	1314
-150	60	2	80:20	1.46	1338
-500	0.5	6	80:20	1.59	1524
-500	10	2	90:10	3.00	1460
-500	60	4	60:40	1.45	1493

Table 8a lists the response table for the signal-to-noise ratio for I_D/I_G ratio based on the Taguchi approach, and Table 8b lists the analysis of variance for I_D/I_G ratio. Table 9a lists the response table for the signal-to-noise ratio for I_D/I_G ratio based on the Taguchi approach, and Table 9b lists the analysis of variance for hardness. Taguchi uses the S/N ratio to measure the quality characteristic deviating from the desired value. There are several S/N ratios available depending on the type of characteristic: smaller is better, nominal is best, and larger is better. In this study, the smaller is better S/N ratio was used for I_D/I_G ratio, larger is better S/N ratio was used for hardness.

Table 8
(a) Response Table for Signal-to-Noise Ratios for ID/IG Ratio

Level	V	F	P	G
1	-3.562	-3.111	-4.526	-1.705
2	-2.994	-6.99	-6.025	-5.869
3	-5.599	-2.053	-1.604	-4.582
Delta	2.605	4.937	4.422	4.164
Rank	4	1	2	3

Table 9
(b) Response table for Signal-to-Noise Ratios for Hardness

Level	V	F	P	G
1	63.77	63.55	63.13	63.14
2	62.77	63.16	63.57	63.33
3	63.48	63.31	63.32	63.54
Delta	0.99	0.39	0.44	0.4
Rank	1	4	2	3

Table 10
(a) ANOVA table for ID/IG Ratio

Factor	Degree of Freedom	Sum of squares	Mean square	Percentage of Contribution (%)
Bias Voltage	2	0.51576	0.25788	9.365
Bias Frequency	2	2.44702	1.22351	44.434
Deposition Pressure	2	1.28862	0.64431	23.399
Gas Composition	2	1.25549	0.62774	22.798
Error	0			
Total	**8**	**5.50689**		**100**

Table 11
(b) ANOVA table for Hardness

Factor	Degree of Freedom	Sum of squares	Mean square	Percentage of Contribution (%)
Bias Voltage	2	42864.2	21432.1	67.653
Bias Frequency	2	6156.2	3078.1	9.716
Deposition Pressure	2	7934.9	3967.4	12.524
Gas Composition	2	6403.6	3201.8	10.105
Error	0			
Total	**8**	**63358.9**		**100**

Figure 10a and Fig. 10b show the main effects plot for S/N ratios. The level of a factor with the highest S/N ratio was the optimum level for the responses measured. From the S/N ratio analysis, the optimal

deposition conditions for I_D/I_G ratio are − 150V bias voltage, 60 kHz bias frequency, 6μbar deposition pressure, and 60:40 gas composition. Similarly, for hardness, these are − 50V bias voltage, 500 Hz bias frequency, 4μbar deposition pressure, and 90:10 gas composition.

It is found that bias frequency has a more significant influence on I_D/I_G ratio, and bias voltage has a more significant impact on hardness. Based on the optimum conditions, experiments were conducted to verify the same for hardness, and the conformance run resulted in a hardness value of 1580 KHN. DLC films were coated at the optimum conditions (-50V bias voltage, 500 Hz bias frequency, 4μbar deposition pressure, and 90:10 gas composition) using Magpuls, i.e., symmetric bipolar power supply on SS wear pins and HSS drill bits. This was done to check the applicability of DLC films for tribological applications.

3.7. Wear and Friction Measurement

Pin-on-disc tests were performed using uncoated SS pins on En31 case-hardened discs. A load of 500 grams, 50 rpm disc speed, and Relative humidity of 40% with variable sliding track radius were used for testing DLC films, and the tests were carried out for 10 mins for uncoated SS pins and 5 mins for coated SS pins.

Figure 11a and Fig. 11b show the uncoated SS pin wear loss in microns and coefficient of friction, respectively. The wear loss of the uncoated SS pin increases over time, and at 300 secs it reaches 14.5 microns. The coefficient of friction reaches up to 0.50 concerning time. Figure 12a and Fig. 12b show the coated SS pin wear loss in microns and coefficient of friction, respectively. Wear loss of coated SS pin was found to be high initially; however, wear loss decreased as time increased, and at 300 secs, wear loss was below 6 microns. The coefficient of friction reaches up to 0.35 concerning time. Figure 13a shows the wear scar of the DLC-coated pin after the wear test. Figure 13b shows the En 31 case-hardened disc where DLC coating is transferred from the pin to the disc.

3.8. Cutting Performance

To study the effect of DLC coating on tool life, uncoated and coated drill bits were tested. Spindle load and drilled hole surface finish were observed for uncoated and coated drill bits. All the drill bits were tested for 60 holes for LM6- aluminum alloy. For bright mild steel, the drills were assumed to have failed when the color of the chip changed to bluish/ golden yellow and the spindle load increased. HSS drill bits were coated by the optimized DLC films with coating parameters of -50V bias voltage, 500 Hz bias frequency, 4μbar deposition pressure, and 90:10 gas composition using a symmetric bipolar power supply. Table 10a and Table 10b show the surface roughness values for drilled holes on LM-6 aluminum alloy and bright mild steel material by uncoated and coated drill bits. It can be observed that coated drill bits show less surface roughness compared to uncoated drill bits. Table 11b and Table 11a show the spindle load values in percentage for drilled holes on LM-6 aluminum alloy and bright mild steel material by uncoated and coated drill bits. It can be observed that coated drill bits show less surface roughness compared to uncoated drill bits.

Table 12
(a) Surface Roughness for holes drilled on LM6-AL alloy

Hole No.	Uncoated Drill bit Ra (μm)	Coated Drill bit Ra (μm)
1st	1.98	1.55
11th	2.52	2.15
22nd	2.47	2.23
33rd	2.37	2.10
44th	2.46	2.21
55th	3.70	2.68
60th	4.49	2.31

Table 13
(b) Surface Roughness for holes drilled on Bright MS

Hole No.	Uncoated Drill bit Ra (μm)	Coated Drill bit Ra (μm)
1st	2.58	1.78
10th	2.79	2.35
20th	3.37	2.80
30th	2.99	2.40
40th	3.23	2.63
50th	3.30	2.55

Table 14
(a) Spindle Load for holes drilled on LM6-AL alloy

Hole No.	Uncoated Drill bit spindle Load (%)	Coated Drill bit spindle Load (%)
1st	20	20
11th	20	20
22nd	22	20
33rd	23	21
44th	23	21
55th	25	21
60th	25	22

Table 15
(b) Spindle Load for holes drilled on Bright mild steel

Hole No.	Uncoated Drill bit spindle Load (%)	Coated Drill bit spindle Load (%)
1st	5	2
10th	5	4
20th	5	3
30th	5	3
40th	5	4
50th	8	4

Figure 14 shows the drill bit geometry before the cutting test. Figure 15 shows the Uncoated Drill geometry after the cutting test on LM-6 Al alloy, and 16 shows the Coated- D108 Drill geometry after the cutting test on LM-6 Al alloy. Tool Makers microscope took all the images at 10X magnification. It is clear from the photo that the uncoated drill bit has more built-up edge formation due to temperature rise during the drilling operation. In case of coated drill built up edge is less compared to the uncoated drill bit due to low coefficient of friction of coating, hence less temperature rise.

Figure 17 shows the Uncoated Drill geometry after the cutting test on Bright MS, and 18 shows the Coated- D114 Drill geometry after the cutting test on Bright MS. All the images were taken by Tool Makers Microscope at 25X magnification. The cutting test was stopped when the color of the chips changed to a bluish/golden yellow color. Uncoated drill bits show wear on the cutting edge and built-up formation at the chisel edge after 50 holes, and at the corner of the drill, catastrophic failure (corner chip off) was observed. Coated drill bits show cutting-edge light wear and built-up formation at the chisel edge after 80 holes; no wear was honored at the drill corner.

Using tool maker's microscope, cutting-edge wear was measured for uncoated and coated drill bits. For uncoated drill bits, cutting edge wear was 0.15 mm / 0.20 mm, and for coated drill bits cutting edge wear was 0.08 mm / 0.14 mm. Drills were not tested to the end of tool life (Defined as tool wear of > 0.3 mm, by ISO 8688-1). Two number drill bits were tested for each drilling conditions/workpiece material combination. Based on the above results, it can be concluded that the coatings improved the surface finish of the drilled holes, and also, the coated drill bits were drawing less power during the operation compared to the uncoated drill bits as judged from lower spindle load. This can be attributed to the lower coefficient of friction of the DLC-coated drills compared to uncoated ones.

4. Conclusion

This study discussed the application of the Taguchi experimental method for investigating the influence of deposition parameters on the properties of Diamond-Like-Carbon (DLC) coatings deposited by Plasma-Enhanced Chemical Vapour Deposition (PECVD). Optimization was carried out for the ID/IG ratio in the

Raman spectrum and hardness of the layers. The DLC films were deposited using the PECVD method with symmetric and asymmetric bipolar pulse biasing on p-type Silicon (100), High-Speed Steel (HSS), SS hemispherical wear pins, and HSS diameter 5 mm drill bits. Based on the results following conclusions can be drawn:

- Taguchi analysis and ANOVA show that bias frequency has a greater influence on ID/IG ratio and bias voltage has a more significant impact on hardness.
- The optimal deposition conditions are − 50V bias voltage, 500 Hz bias frequency, 4μbar deposition pressure & 90:10 gas composition for hardness. A conformance test was carried out at optimum conditions, resulting in a hardness value of 1580 KHN.
- The FT-IR results revealed that DLC films were partially hydrogenated, consisting of various sp^3 and sp^2-related C-H bonds.
- Residual stresses in DLC films can be both tensile and compressive in nature.
- AFM images show that the DLC films are smooth with a roughness Ra ranging from 6.9 nm to 9.0 nm on a silicon substrate.
- Wear and Friction tests using a Pin-On-Disc wear tester show a low coefficient of friction, i.e., 0.33, and wear loss of up to 6 microns.
- Cutting tests were performed on LM6-aluminum alloy and Bright mild steel for uncoated and coated drill bits to study the effect of DLC coating on the tool life. Coated drill bits produce a better finish in terms of surface roughness and consume less power during the drilling operation than uncoated drill bits.

Declarations

Credit authorship contribution statement:

VSJ, **EMS**, **AVJ**, **AM**, **RDD**: Conceptualization, Methodology, writing an original draft, making simulation, review & editing the whole paper. All authors have read and agreed to the published version of the manuscript.

Funding

This research did not receive any specific grant from funding agencies in the public, commercial, or not-for-profit sectors.

Declaration of competing interest

The authors declare that they have no competing personal and financial interests.

Data availability

Not applicable.

Code availability

Not applicable

Ethics approval

Not applicable.

Consent to participate

Not applicable.

Consent for publication

Not applicable

References

1. Donnet C, Erdemir A (2007) Tribology of diamond-like carbon films: fundamentals and applications. Springer Science & Business Media
2. Erdemir A, Donnet C "Tribology of diamond-like carbon films: recent progress and future prospects," *Journal of Physics D: Applied Physics*, vol. 39, no. 18, p. R311, 2006/09/01 2006, doi: https://doi.org/10.1088/0022-3727/39/18/R01
3. Conrads H, Schmidt M (2000) "Plasma generation and plasma sources,". Plasma Sources Sci Technol 9(4):441. https://dx.doi.org/10.1088/0963-0252/9/4/301. /11/01 2000, doi
4. Psyllaki PP, Jeandin M, Pantelis DI, Allouard M (2000) Pin-on-disc testing of PE-CVD diamond-like carbon coatings on tool steel substrates,. Surf Coat Technol 130(2):297–303. doi: https://doi.org/10.1016/S0257-8972(00)00711-8. 2000/08/21/
5. Dorner A, Schürer C, Reisel G, Irmer G, Seidel O, Müller E (2001) "Diamond-like carbon-coated Ti6Al4V: influence of the coating thickness on the structure and the abrasive wear resistance," *Wear*, vol. 249, no. 5, pp. 489–497, /06/01/ 2001, doi: https://doi.org/10.1016/S0043-1648(01)00587-7
6. Pauschitz A, Schalko J, Koch T, Eisenmenger-Sittner C, Kvasnica S, Roy M (2003) Nanoindentation and AFM studies of PECVD DLC and reactively sputtered Ti containing carbon films,. Bull Mater Sci 26(6):585–591. https://doi.org/10.1007/BF02704320. /10/01 2003, doi
7. Y. KAGIYA, "Development of DLC coating film (AURORACOAT) and its application to tools,"SEI Technical review, vol. 55, pp.89–94,
8. Fukui H, Okida J, Omori N, Moriguchi H, Tsuda K "Cutting performance of DLC coated tools in dry machining aluminum alloys,"Surface and Coatings Technology, vol. 187, no. 1, pp.70–76, 2004/10/01/ 2004, doi: https://doi.org/10.1016/j.surfcoat.2004.01.014
9. Lee JJ (2005) "Application of inductively coupled plasma to CVD and PVD,". Surf Coat Technol 200(1):31–34. https://doi.org/10.1016/j.surfcoat.2005.02.113. 10/01/ 2005, doi

10. Irmer G, Dorner-Reisel A (2005) "Micro-Raman studies on DLC coatings,". Adv Eng Mater 7(8):694–705. doi: https://doi.org/10.1002/adem.200500006
11. Zaidi H, Djamai A, Chin KJ, Mathia T "Characterisation of DLC coating adherence by scratch testing,"Tribology International, vol. 39, no. 2, pp.124–128, 2006/02/01/ 2006, doi: https://doi.org/10.1016/j.triboint.2005.04.016
12. Bhowmick S, Alpas AT "The performance of hydrogenated and non-hydrogenated diamond-like carbon tool coatings during the dry drilling of 319 Al,"International Journal of Machine Tools and Manufacture, vol. 48, no. 7, pp.802–814, 2008/06/01/ 2008, doi: https://doi.org/10.1016/j.ijmachtools.2007.12.006
13. Zolgharni M, Jones BJ, Bulpett R, Anson AW, Franks J "Energy efficiency improvements in dry drilling with optimised diamond-like carbon coatings,"Diamond and Related Materials, vol. 17, no. 7, pp.1733–1737, 2008/07/01/ 2008, doi: https://doi.org/10.1016/j.diamond.2007.11.012
14. Dowling D (2008) "Metal finishing: enhanced performance achieved through plasma processing,". Trans IMF 86(3):136–140. https://doi.org/10.1179/174591908X264310. /05/01 2008, doi
15. Cao N et al "Characterization and tribological application of diamond-like carbon (DLC) films prepared by radio-frequency plasma-enhanced chemical vapor deposition (RF-PECVD) technique,"Frontiers of Materials Science in China, vol. 3, no. 4, p.409, 2009/10/20 2009, doi: https://doi.org/10.1007/s11706-009-0070-8
16. Heinemann RK, Hinduja S "Investigating the feasibility of DLC-coated twist drills in deep-hole drilling,"The International Journal of Advanced Manufacturing Technology, vol. 44, no. 9, p.862, 2009/01/13 2009, doi: https://doi.org/10.1007/s00170-008-1912-8
17. Suzuki A, Aiyama Y, Tokoro M, Sekiguchi H, Masuko M "Friction and wear characteristics of hydrogenated diamond-like carbon films formed on the roughened stainless steel surface," *Wear*, vol. 269, no. 1, pp. 118–124, 2010/05/20/ 2010, doi: https://doi.org/10.1016/j.wear.2010.03.013
18. Bhowmick S, Alpas AT "The role of diamond-like carbon coated drills on minimum quantity lubrication drilling of magnesium alloys,"Surface and Coatings Technology, vol. 205, no. 23, pp.5302–5311, 2011/09/25/ 2011, doi: https://doi.org/10.1016/j.surfcoat.2011.05.037
19. Kumar MA, Fujii M, Fukuda T (2012) Tribological characteristics of DLC coatings in vacuum under sliding contact,. J Surf Eng Mater Adv Technol 2(1):22–27. doi: https://DOI.org/10.4236/jsemat.2012.21004
20. Pang X, Peng H, Yang H, Gao K, Wu X, Volinsky AA (2013) Fast deposition of diamond-like carbon films by radio frequency hollow cathode method,. Thin Solid Films 534:226–230 2013/05/01/. doi: https://doi.org/10.1016/j.tsf.2013.02.123
21. Bewilogua K, Hofmann D (2014) "History of diamond-like carbon films — From first experiments to worldwide applications,". Surf Coat Technol 242:214–225. https://doi.org/10.1016/j.surfcoat.2014.01.031. 03/15/ 2014, doi
22. Waseem B et al "Optimization and Characterization of Adhesion Properties of DLC Coatings on Different Substrates," *Materials Today: Proceedings*, vol. 2, no. 10, Part B, pp. 5308–5312,

2015/01/01/ 2015, doi: https://doi.org/10.1016/j.matpr.2015.11.041

23. Hauert R (2004) "An overview on the tribological behavior of diamond-like carbon in technical and medical applications,". Tribol Int 37(11):991–1003. https://doi.org/10.1016/j.triboint.2004.07.017. 11/01/ 2004, doi
24. Ye Y, Wang Y, Ma X, Zhang D, Wang L, Li X "Tribocorrosion behaviors of multilayer PVD DLC coated 304L stainless steel in seawater,"Diamond and Related Materials, vol. 79, pp.70–78, 2017/10/01/ 2017, doi: https://doi.org/10.1016/j.diamond.2017.09.002
25. Bouabibsa I, Lamri S, Alhussein A, Minea T, Sanchette F "Plasma investigations and deposition of Me-DLC (Me = Al, Ti or Nb) obtained by a magnetron sputtering-RFPECVD hybrid process,"Surface and Coatings Technology, vol. 354, pp.351–359, 2018/11/25/ 2018, doi: https://doi.org/10.1016/j.surfcoat.2018.09.033
26. Liu JQ, Li LJ, Wei B, Wen F, Cao HT, Pei YT (2019) Effect of sputtering pressure on the surface topography, structure, wettability and tribological performance of DLC films coated on rubber by magnetron sputtering,. Surf Coat Technol 365:33–40. https://doi.org/10.1016/j.surfcoat.2018.05.012. /05/15/ 2019, doi
27. Guo C-Q et al "Modulation of Si on microstructure and tribo-mechanical properties of hydrogen-free DLC films prepared by magnetron sputtering,"Applied Surface Science, vol. 509, p.145381, 2020/04/15/ 2020, doi: https://doi.org/10.1016/j.apsusc.2020.145381
28. Claver A et al "Comparative Study of Tribomechanical Properties of HiPIMS with Positive Pulses DLC Coatings on Different Tools Steels," *Coatings*, vol. 11, no. 1, p. 28, 2021. [Online]. Available: https://www.mdpi.com/2079-6412/11/1/28
29. Bai C, Qiang L, Zhang B, Gao K, Zhang J "Optimizing the tribological performance of DLC-coated NBR rubber: The role of hydrogen in films," *Friction*, vol. 10, no. 6, pp. 866–877, 2022/06/01 2022, doi: 10.1007/s40544-021-0498-0
30. Delplancke-Ogletree M-P, Monteiro OR "In situ measurement of stresses in diamond-like carbon films,"Diamond and Related Materials, vol. 12, no. 12, pp.2119–2127, 2003/12/01/ 2003, doi: https://doi.org/10.1016/S0925-9635(03)00240-1
31. Methods AT (2011) "Standard Test Method for Wear Testing with a Pin-on-Disk Apparatus1," *Wear*, vol. 5, pp. 1–5,

Figures

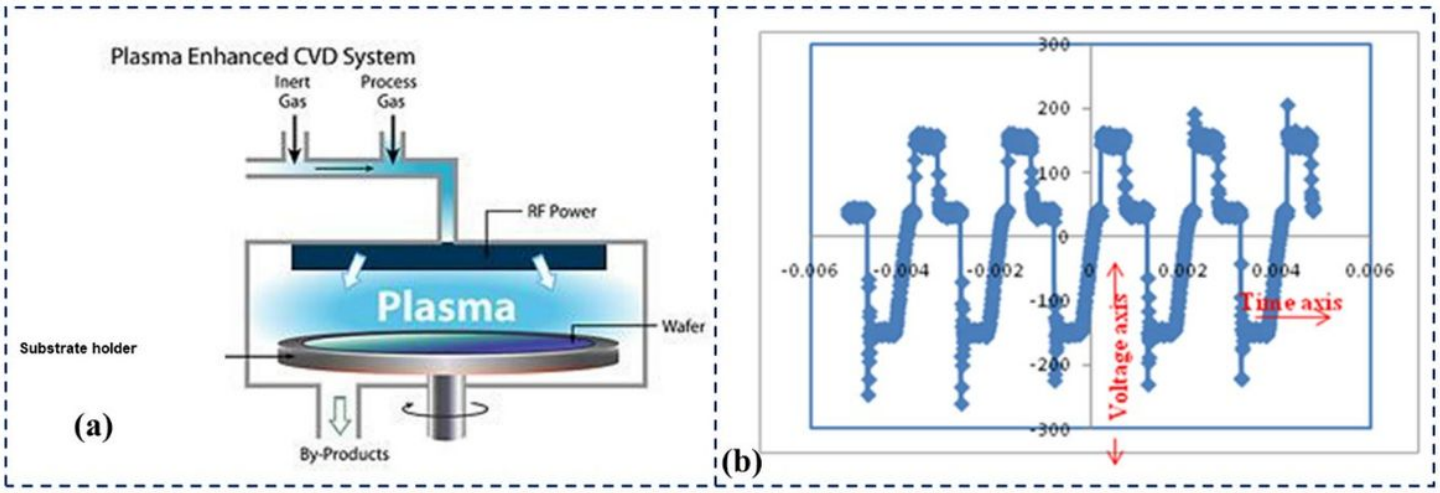

Figure 1

schematic of the PECVD system (b) Symmetric bipolar pulse waveform of Magpuls Power Supply

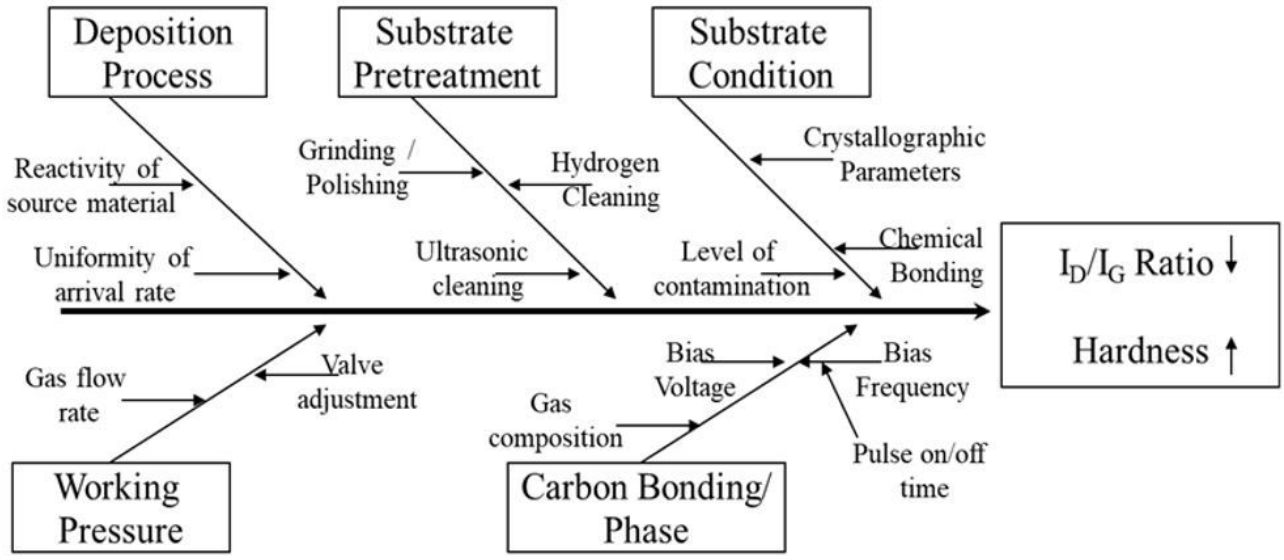

Figure 2

Cause and Effect Diagram for DLC film

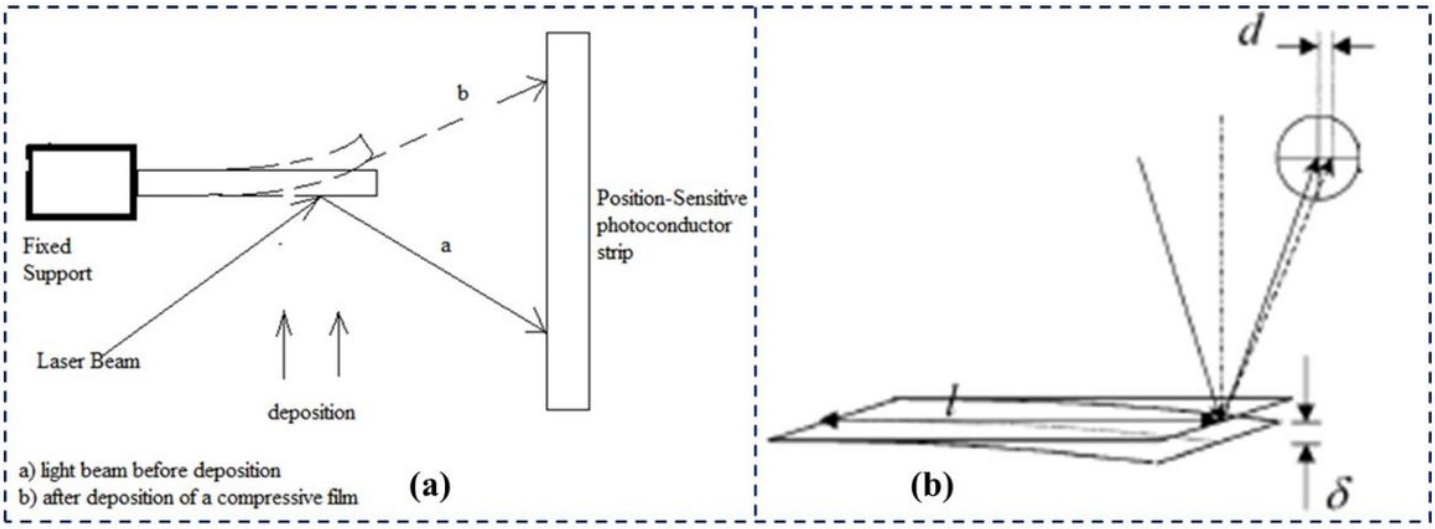

Figure 3

(a) Technique for measuring intrinsic stress (b) stress measurement [30]

Figure 4

Drilling Experimental Setup

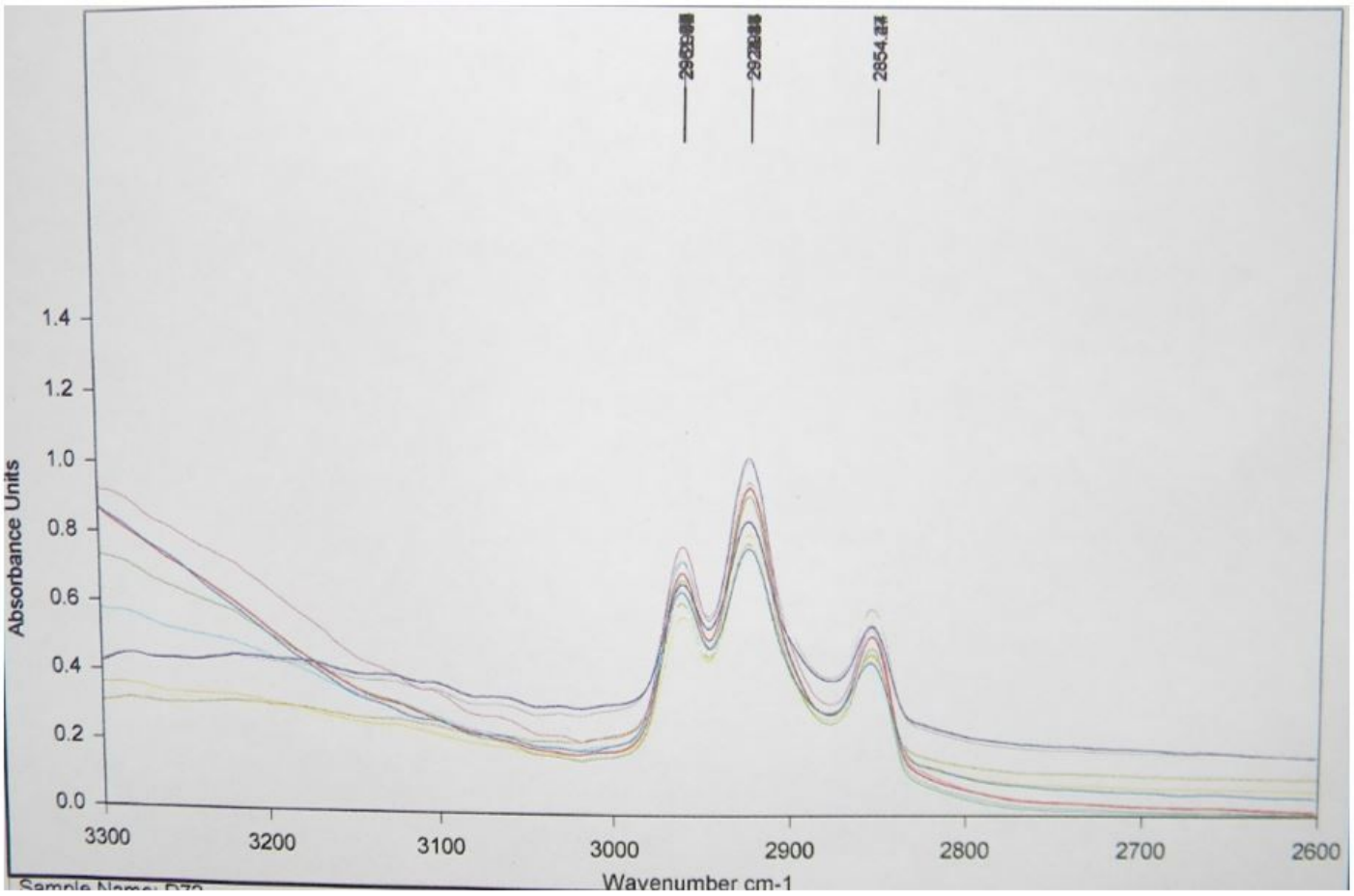

Figure 5

FTIR Spectra of DLC films

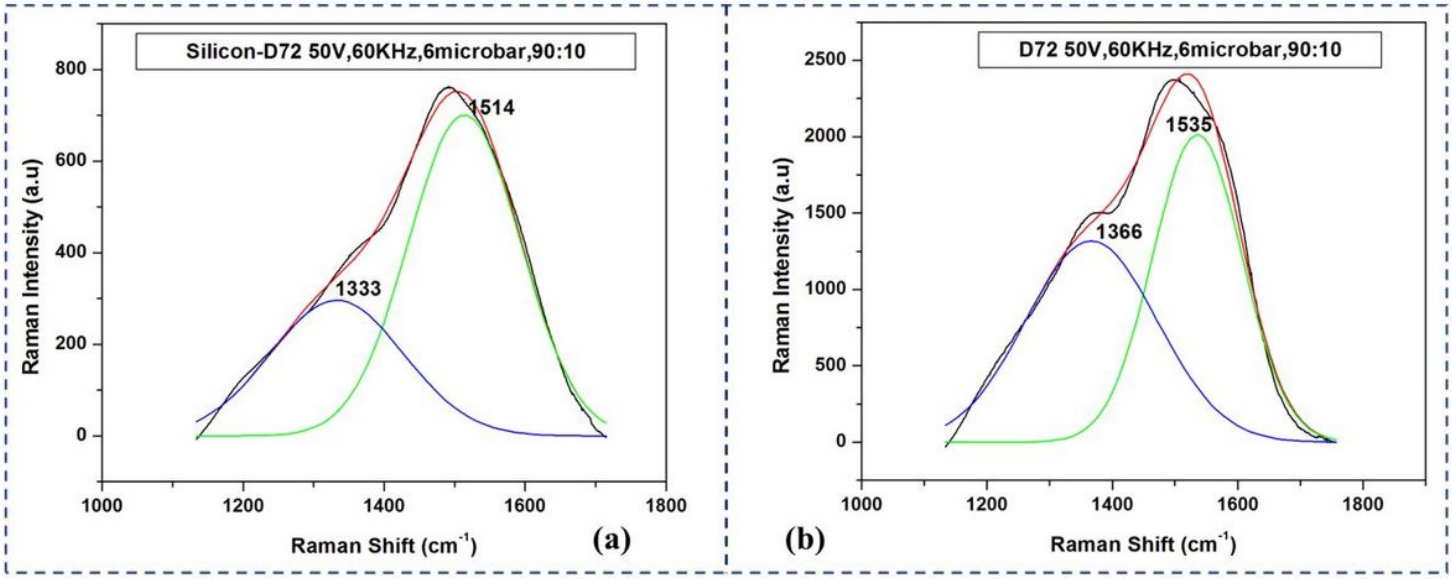

Figure 6

(a) Raman Spectrum of DLC film coated on Silicon substrate (b) Raman Spectrum of DLC film coated on HSS substrate

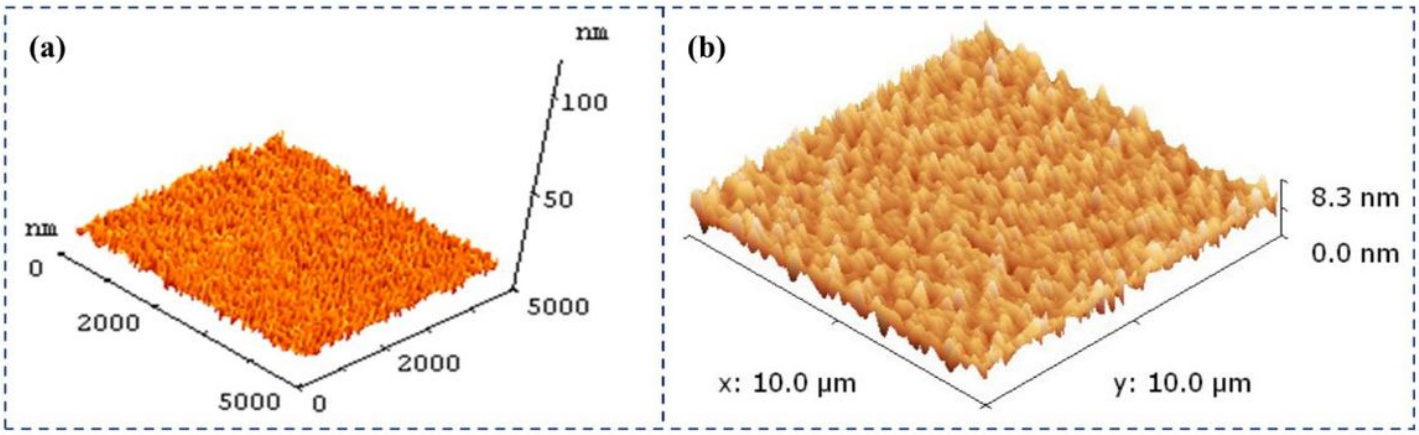

Figure 7

(a) AFM image of the bare silicon substrate (b) AFM image of DLC coating on a silicon substrate

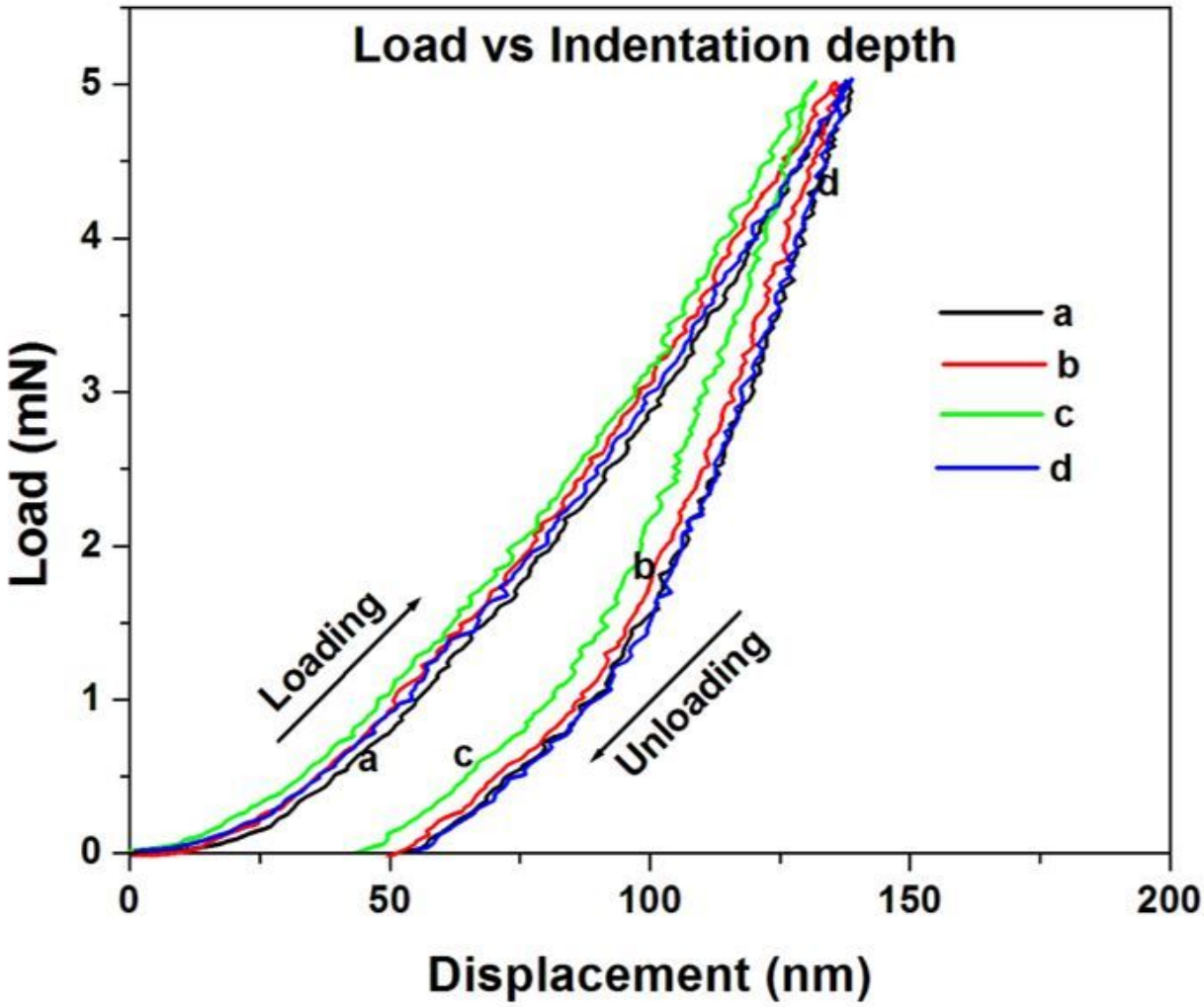

Figure 8

Indentation curve for DLC film deposited on Silicon

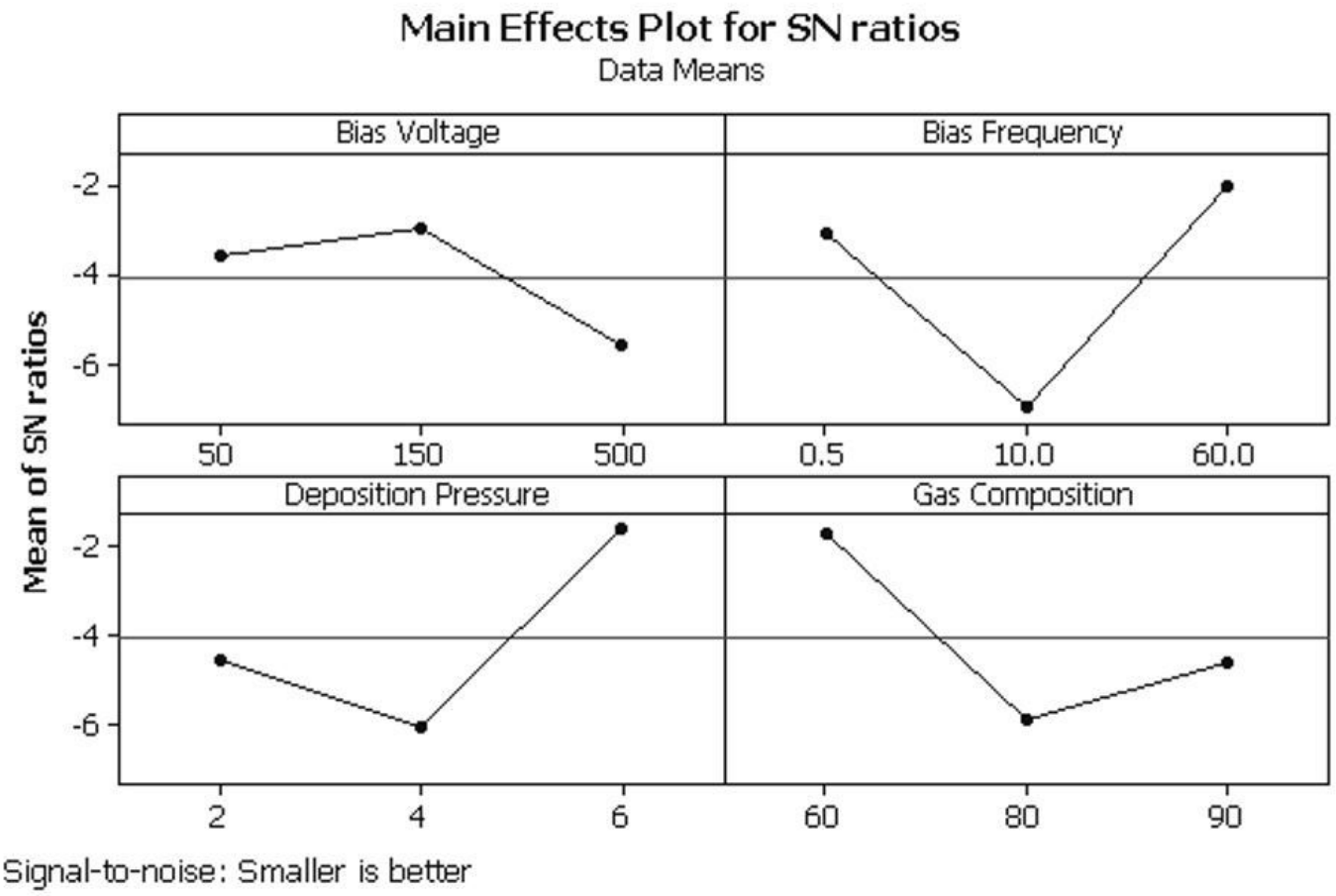

Figure 9

(a) S/N ratio values for ID/IG ratio

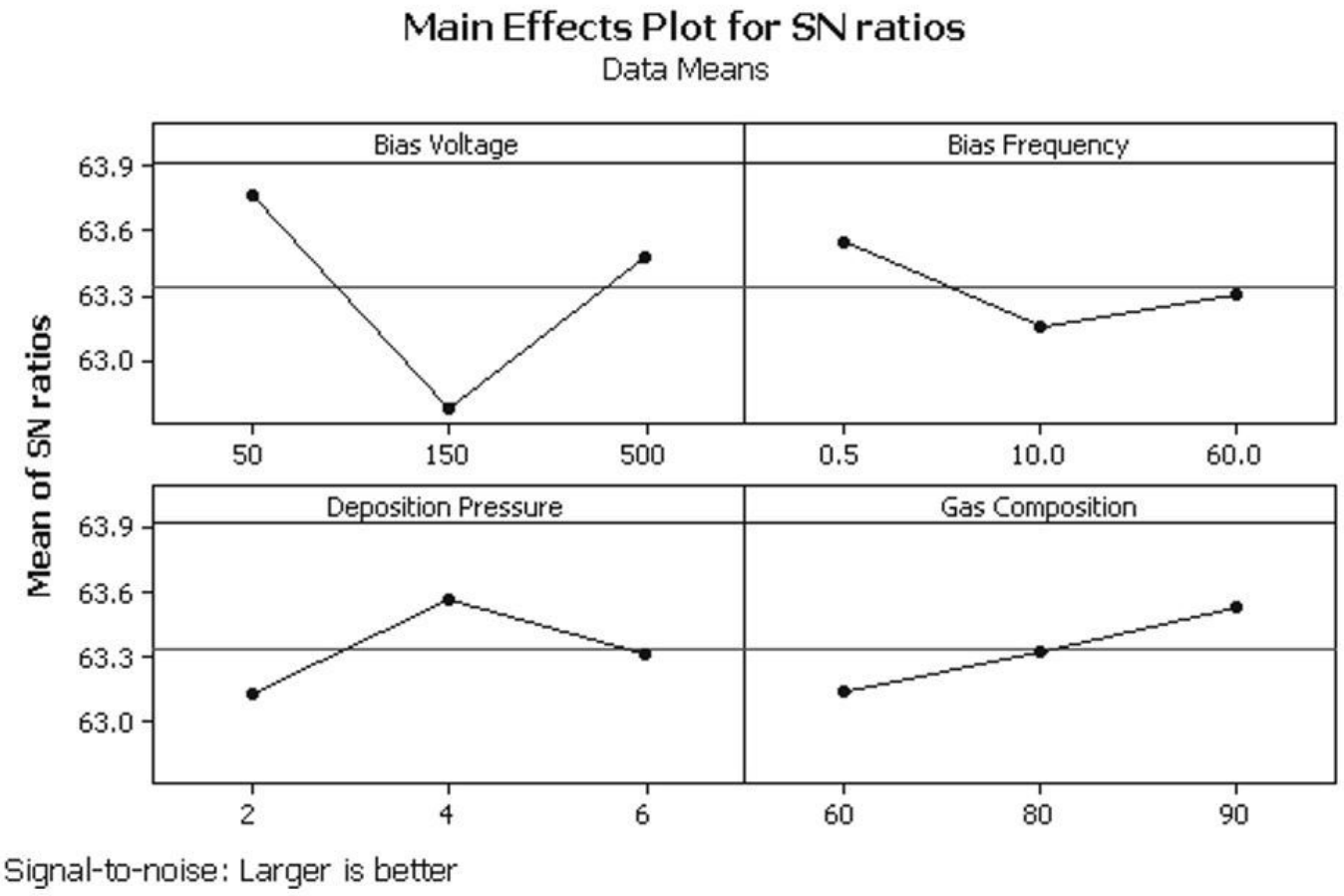

Figure 10

(b) S/N ratio values for Hardness

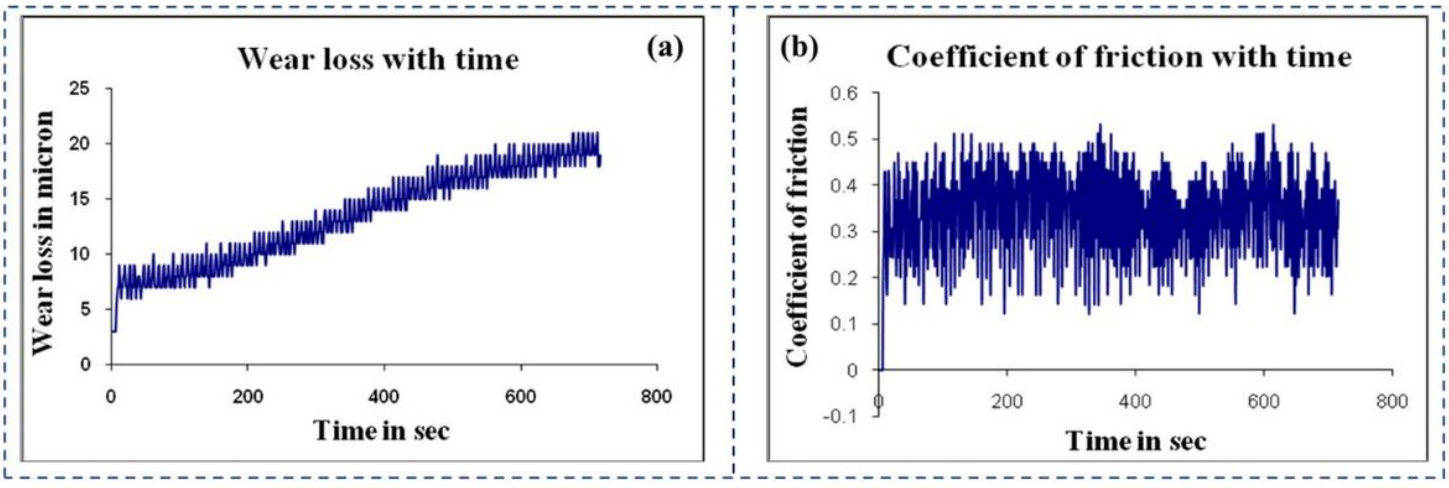

Figure 11

(a) Wear loss of uncoated SS pin (b) CoF loss of uncoated SS pin

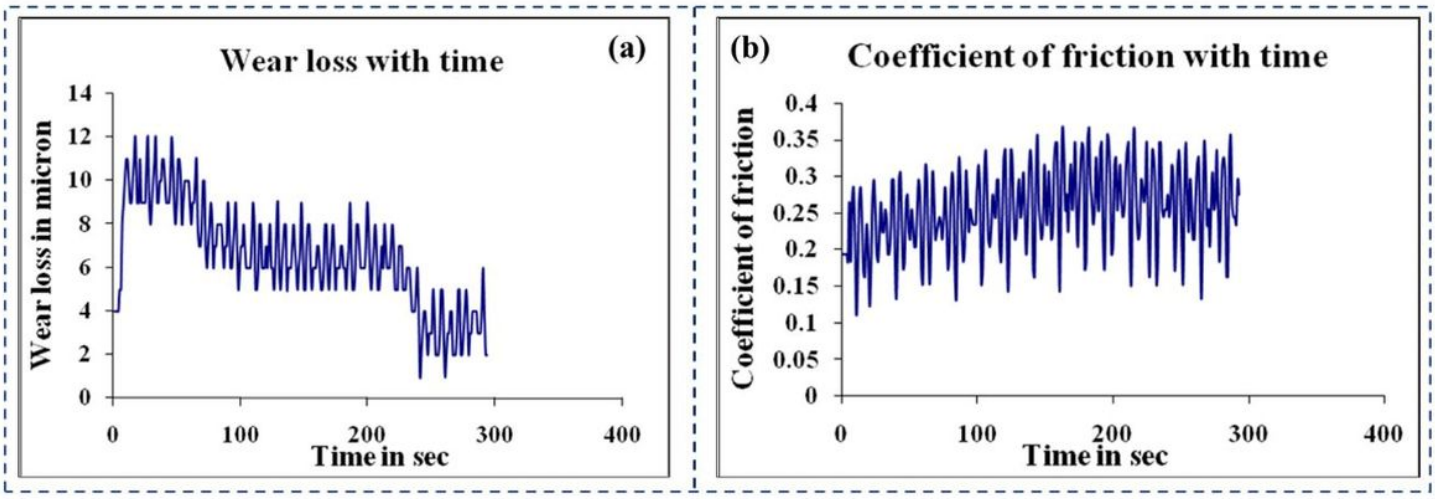

Figure 12

(a) Wear loss of coated SS pin (b) CoF of coated SS pin

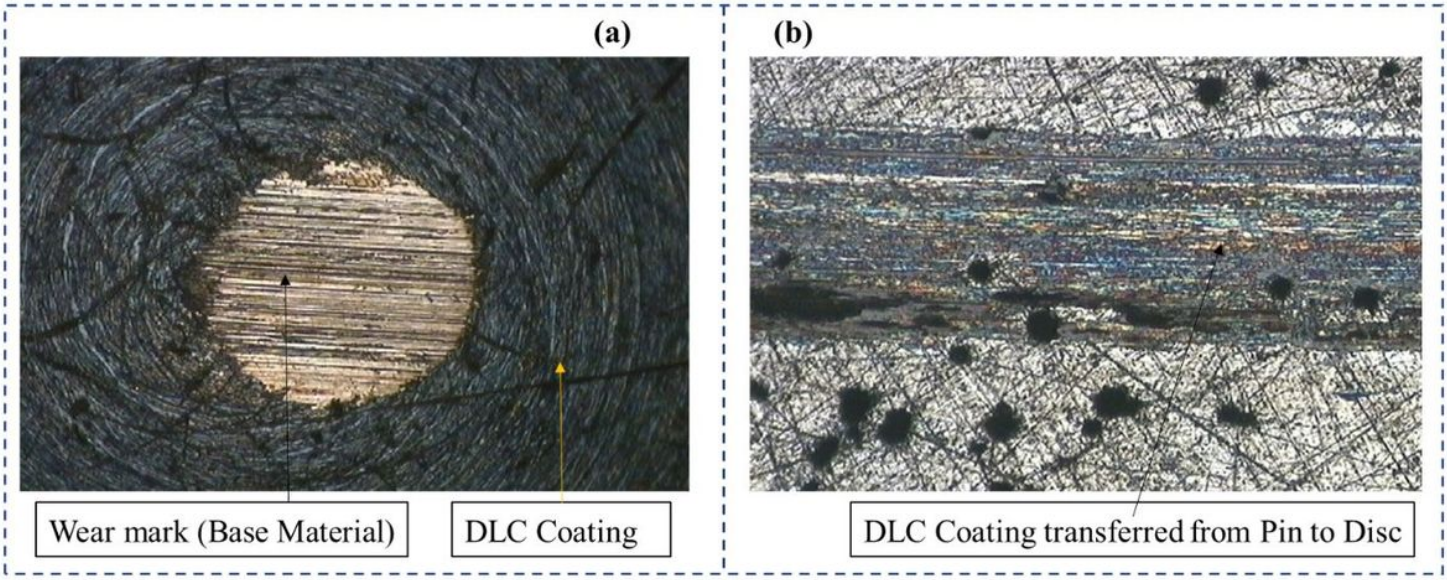

Figure 13

(a) Wear scar on DLC Coated SS Pin at 50X magnification (b) En31 case-hardened disc at 50X magnification

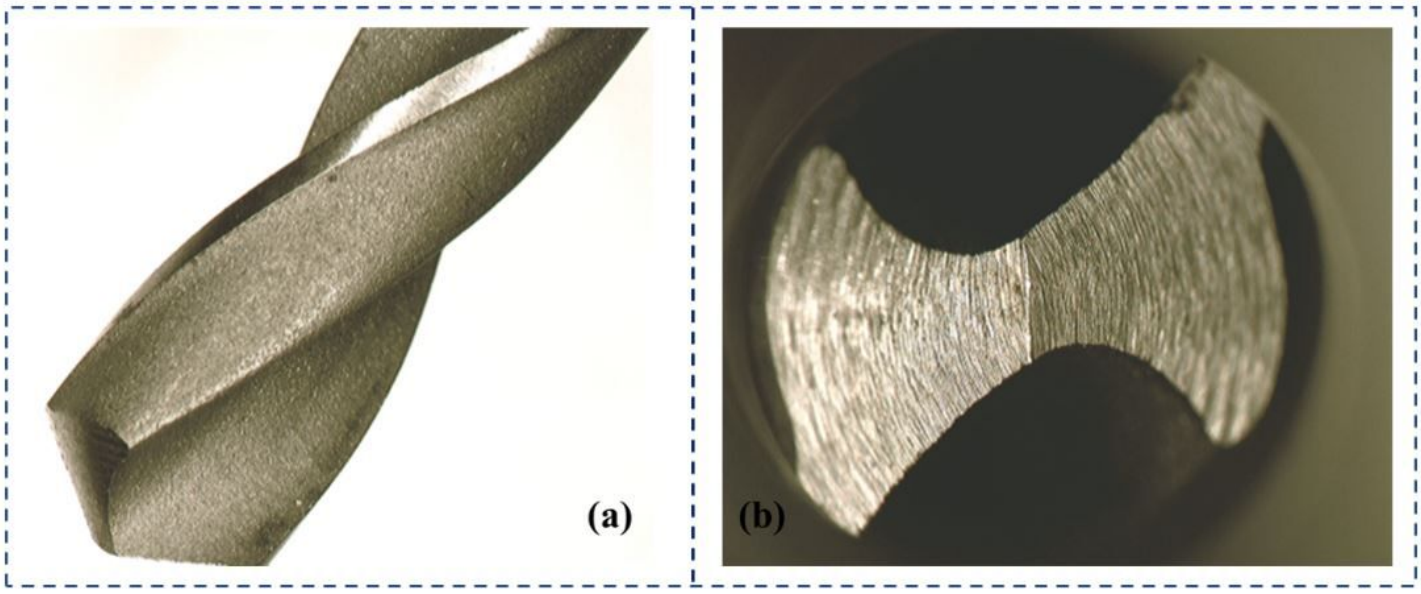

Figure 14

Drill geometry before cutting test

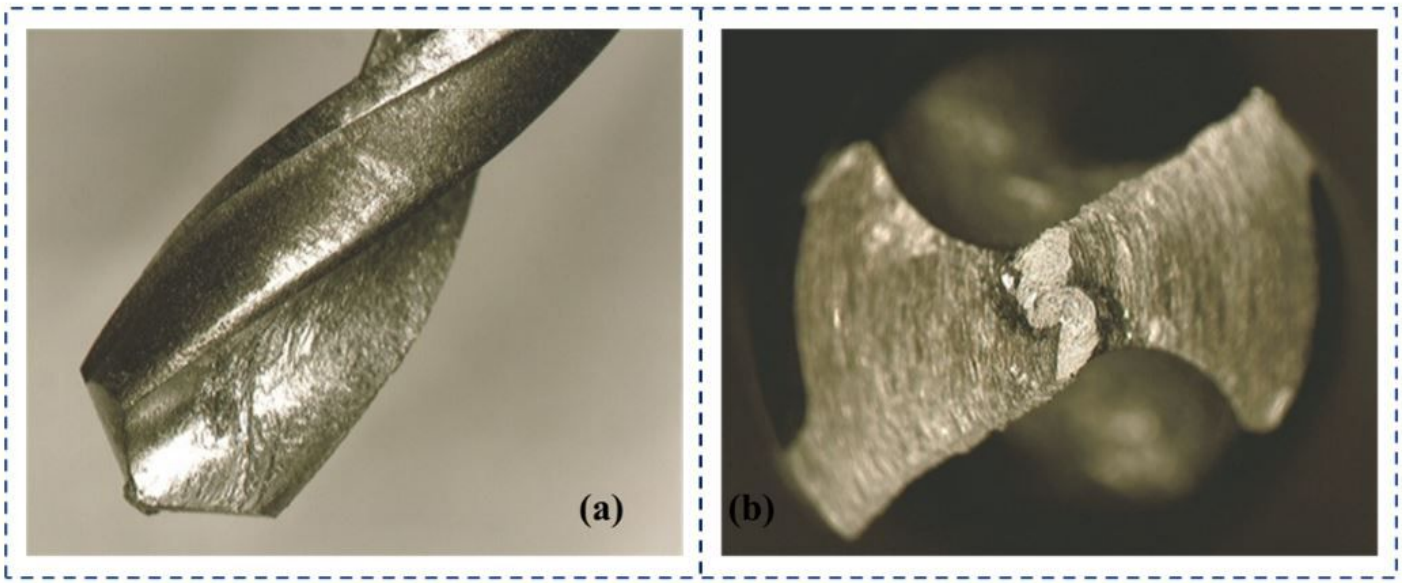

Figure 15

Uncoated Drill geometry after cutting test on LM-6

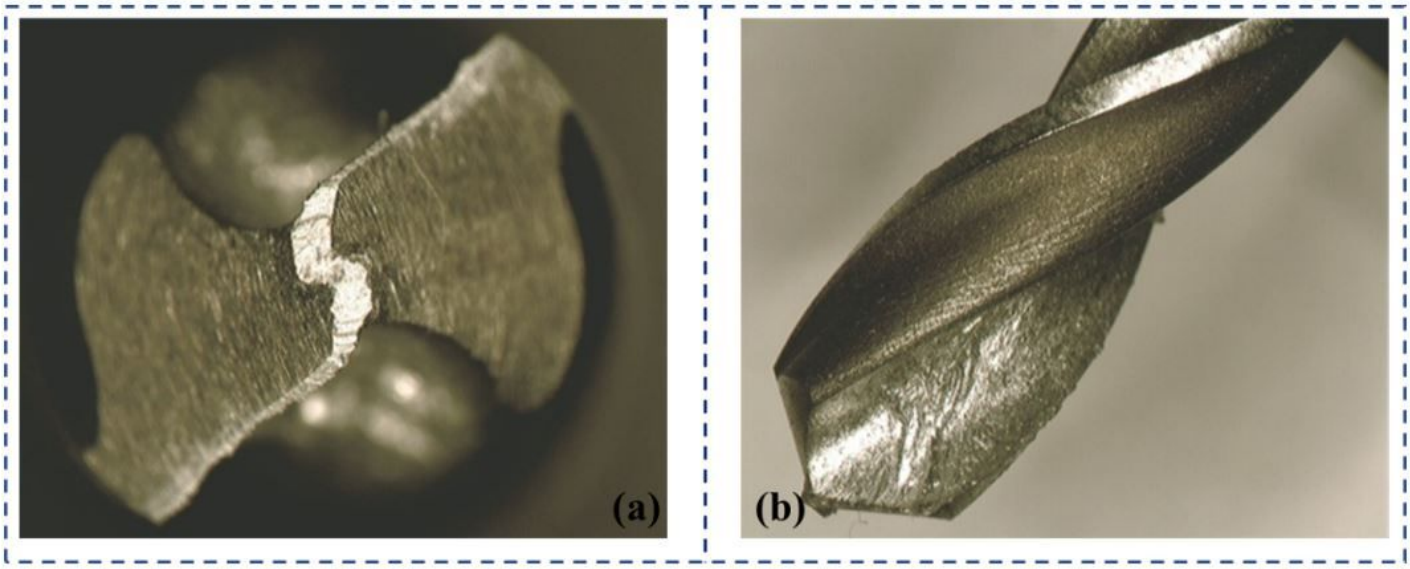

Figure 16

Coated Drill geometry after cutting test on LM-6

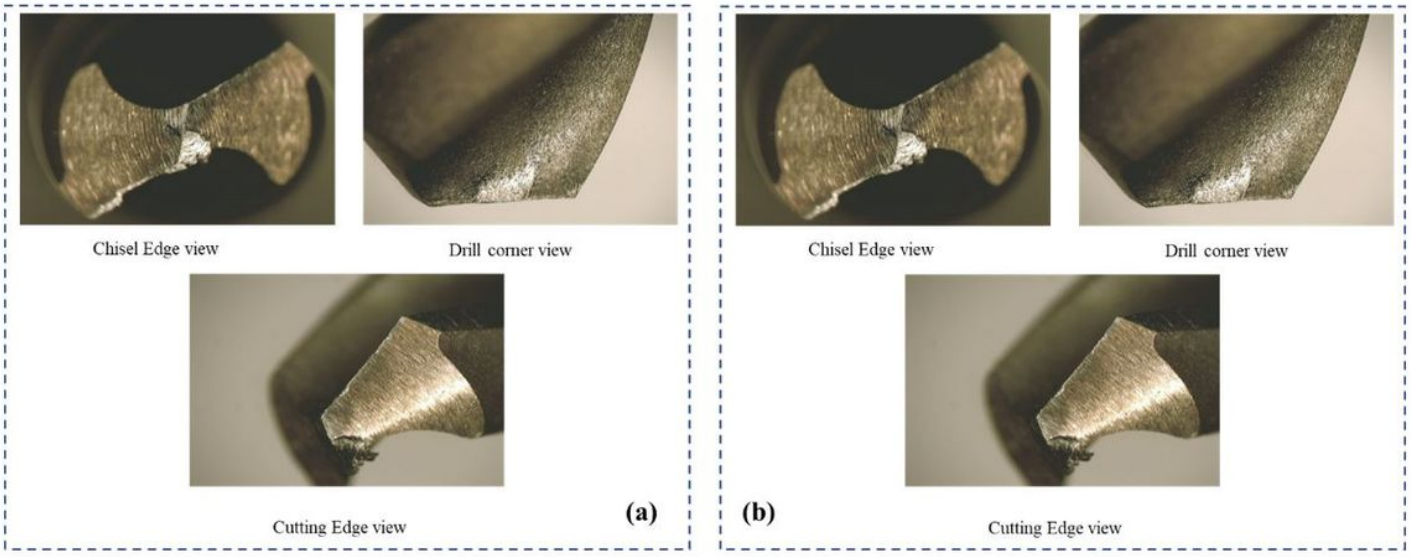

Figure 17

(a) Uncoated Drill geometry after cutting test on Bright MS (b) Coated- D114 Drill geometry after cutting test on Bright MS